L-VALVE DESIGN STUDY FOR A CONTINUOUS TEMPERATURE SWING ADSORPTION CO2 CAPTURE UNIT

Egon Zehetner*, Gerhard Schöny, Hermann Hofbauer

TU Wien, Institute of Chemical Engineering, Getreidemarkt 9/166, 1060 Vienna, Austria

** Email:egon.zehetner@tuwien.ac.at*

ABSTRACT

A fluid-dynamic cold flow study was carried out to assess the suitability of L-Valves as control device for the sorbent circulation rate within a recently proposed temperature swing adsorption (TSA) CO_2 capture system that consists of interconnected multi-stage fluidized bed columns. The cold flow model used in this work comprises a stationary fluidized bed and a solids recirculation system. The recirculation system itself consists of an L-Valve that extracts bed material from the bottom of the fluidized bed at a controlled rate and a pneumatic transport riser that redirects the material back onto the top of the fluidized bed. The aim of this work was to investigate the L-Valve transport behaviour and operating range under different pressure conditions. Furthermore, the leakage of fluidization gas from the main fluidized bed into the recirculation system was measured by using propane as tracer gas. Finally, the utilization of purge gas, introduced in the upper section of the L-Valve standpipe, was tested as gas sealing measure. It was found, that for specific operating conditions the L-Valve aeration itself prevents gas leakage into the recirculation system. However, for all other operating conditions it was necessary to introduce purge gas in order to prevent gas slip. Results from this work clearly demonstrate that L-Valves are suitable sorbent circulation control devices for continuous TSA systems if they are used in combination with purge gas streams for prevention of gas slip between the adsorber and the desorber.

1. INTRODUCTION

Temperature swing adsorption (TSA) systems have recently been proposed as cost efficient alternative to amine scrubbing systems for continuous post combustion CO_2 capture applications. Among the proposed TSA reactor designs, those that incorporate multistage fluidized bed columns as gas solid contactors seem to be superior to other design solutions (Krutka et al., 2013; Nelson et al., 2014). Most recently, authors of this work introduced a bench scale unit based on such a system. A basic scheme of this unit is shown in Fig. 1. Both columns, namely the adsorber and the desorber consist of five consecutive bubbling fluidized bed stages to achieve counter current contact of gas and solids. Each stage has a perforated plate type gas distributor and the solids transport from stage to stage is realized by overflow downcomers. Heat exchangers immersed in the fluidized beds are used either for cooling in the adsorber column or heating in the desorber column to maintain the required stage temperatures for the temperature swing adsorption process. In the adsorber column flue gas or synthetic gas mixtures with different contents of nitrogen, oxygen and CO2 can be used to fluidize the column, whereas in the desorber column steam or nitrogen or a mixture of both is used as stripping and fluidization gas. The solids transport between the adsorber and the desorber is facilitated by two individual transport lines. In both transport lines the solids are extracted from the bottom of the lowermost stage by a L-valves and are transported to a pneumatic transport riser, which is lifting the solids above the columns. A riser pot installed at the bottom of the riser can be used to realize pre-heating and cooling of the solids. At the top of each riser, a gas-solids separator is installed and solids are separated from the transport gas of the riser and redirected to the top stage of the respective column. The transport gas exits the gas-solid separator at the top and gets recycled to the bottom of the transport risers. During the experiment, the solids circulation rate is calculated from the pressure drop over the risers. More detailed information on the bench scale unit process setup and design parameters can be found elsewhere (Pröll et al., 2016; Schöny, Zehetner et al., 2016; Schöny, Dietrich et al. 2016).

In the present process, L-Valves are used to control the solids circulation rate. Due to their cheap construction, long maintenance intervals and low particle attrition compared to mechanical transport systems, they are the preferred transport option for this process. The transport behaviour for various solids and design aspects were investigated by different researchers (Arena, Langeli, & Cammarota, 1998; Geldart & Jones, 1991; Knowlton & Hirsan, 1978) and equations for the L-Valve operation parameters were developed (Arena et al., 1998; Chovichien et al., 2013; Yang & Knowlton, 1993). However, besides the control of the solids circulation rate the transport system has to meet a further requirement. For utilization or storage of the captured CO_2, high demands on the purity have to be fulfilled. For transport, pipelines are commonly used and several suggestions were made to establish purity standards for the CO_2 product.

Impurities have not only an effect on the energy requirements for compression, but can also lead to severe corrosion of the pipelines (Sim et al., 2014). Therefore, minimum specification requirements were made for the composition of the CO_2 product ((Forbes et al., 2008; *IPCC Special Report on Carbon Dioxide Capture and Storage*, 2005), with recommended oxygen limits in the ppm range. This is challenging for a post combustion CO_2 capture process, where usually flue gases with a significant oxygen contents are treated. In the present case, the gas slip from the adsorber column via the L-Valve to the riser system has to be eliminated. The gas flow in L-Valves was investigated in detail by other researchers (Yazdanpanah et al., 2012; Yazdanpanah IFP et al., 2013) and it can be assumed, that for certain operating and pressure conditions no gas slip between column and riser system occurs. However, the gas flow and pressure conditions are strongly influenced by the solids circulation in the present system and to achieve gas sealing for different operation conditions, a gas purge in the top section of the L-Valve will be tested.

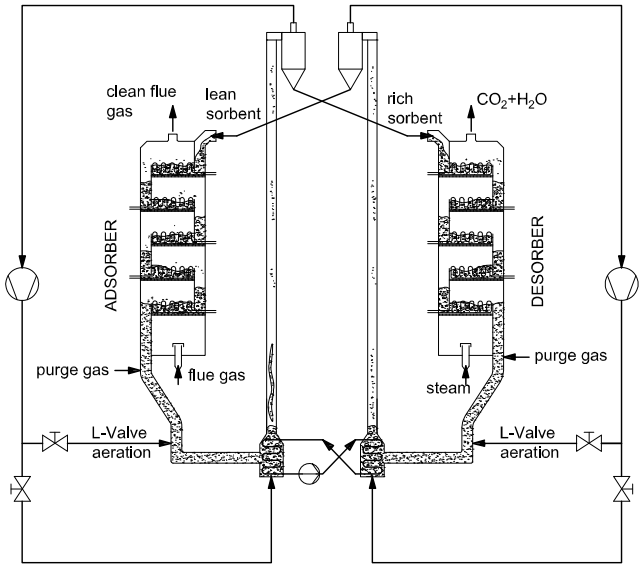

Fig. 1 Temperature swing adsorption process for continuous CO_2 capture

2. EXPERIMENTAL

COLD FLOW MODEL SETUP

The cold flow model used in this work is shown in Fig. 2. The cross section of the column (a) is 220 by 220 mm at an overall height of one meter. The column is mostly made out of Perspex to allow for visual observation of the bubbling fluidized bed (3). The height of the freeboard (4) is sufficient to prevent entrainment of the bed material. To reduce electrostatic effects during operation, all metal parts such as the gas distributor, the riser and the L-Valve have been grounded and the fluidization air is humidified prior introduction into the unit. The humidified air enters the windbox (1) at the bottom of the column, where it passes through the gas distributor plate (2). To avoid solids falling into the windbox, bubble caps were used for gas distribution. The solids are extracted at the bottom of the fluidized bed via a 45 degree inclined pipe section into the recirculation system (b) that redirects the particles to the top of the column. The recirculation system itself consists of a L-Valve (5), a pneumatic riser with a riser pot (6) and a transport section (7) and a gravitational gas-solids separator (8). The inner diameter of the L-Valve and the transport section in the riser was 26 mm. As found out in initial L-Valve design studies (Knowlton & Hirsan, 1978), the optimum location of the aeration tap is above, but close to the center line of the horizontal leg. Thus, the aeration tap was positioned 25 mm above the horizontal section. Before entering the column, the solids pass a cylindrical vessel (9) of known volume which can be closed at the outlet during operation. By measuring the time it takes the solids to fill the vessel, the solids circulation rate can be determined without opening the system and with minor changes to the pressure profile within the unit.

For monitoring of the solids distribution within the unit, pressure taps (p1-p7) were installed in all places of interest, e.g. in several sections of the L-Valve, in the fluidized bed column and along the transporting section of the riser. For measuring the gas slip between the column and the recirculation system, a tracer gas

was added to the column aeration and a measurement tap for a flame ionisation detector was installed in the transport section of the riser. To reduce the gas slip from the column into the recirculation system, a purge gas tap (10) was installed in the top section of the standpipe.

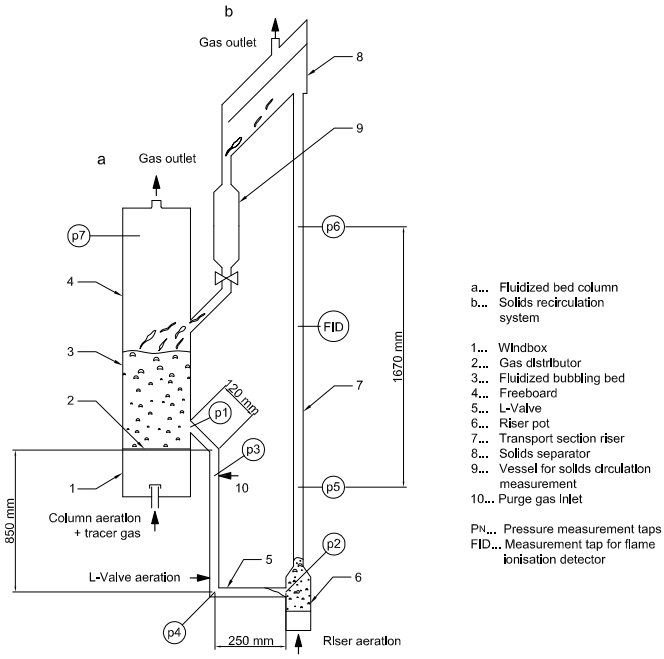

Fig. 2 *Cold flow model setup*

MEASURING EQUIPMENT

The pressure measurement has been performed via Kalinsky DS2 differential pressure sensors. The pressure sensors were connected to the unit's pressure taps via silicon tubes. The linearity error of the applied sensors is less than or equal to 1 % of full scale. All reported pressure values have been averaged over at least 2 min after steady state conditions were reached to compensate fluctuations in the pressure signals.

Leakage tests were performed with a flame ionisation detector (FID), type TESTA 1230. During these tests, the supply air for the column fluidization was mixed with a tracer gas to reach a concentration of 1 %. For this purpose, propane with a purity over 99.5 % was used. The FID was calibrated with a test gas containing 80 ppm propane, which was in the range of the expected concentrations in the riser. To ensure constant air and tracer gas flows, the temperature of the supply air was measured in the windbox of the column and the line pressure for both tracer gas and air was monitored and adjusted by pressure regulators. The air and tracer gas supply in all areas of the model were set by variable area flowmeters, type Krohne VA40 and Krohne DK48. Both types have a measurement accuracy of 1 percent relative to full scale value.

BED MATERIAL

For this experimental campaign, a bed material of the Geldart Group B (Geldart, 1973) was used. Initial leakage tests with a sorbent material for CO_2 capture showed an adsorption of the tracer gas which effected the accuracy of the measurements. Thus, the bed material was replaced by inert polystyrene beads with similar fluid dynamic properties as shown in Table 1. The bulk density as well as the minimum fluidization velocity were determined experimentally in separate test rigs.

Table 1 Fluid dynamic parameters bed material

Parameter	Unit	value
material	-	polystyrene
d_{sv}	µm	870
ρ_p	$kg \cdot m^{-3}$	1040
ρ_b	$kg \cdot m^{-3}$	600
ε_{mf}	-	0.42
U_{mf}	$m \cdot s^{-1}$	0.25

EXPERIMENTAL PROCEDURE

The fluidization gas supply within the bubbling bed column was set to 70 $Nm^3 \cdot h^{-1}$, which corresponds to a fluidization number U/U_{mf} of 1.6. The riser was operated with an aeration of 14 $Nm^3 \cdot h^{-1}$ which results in a superficial gas velocity of 7.3 $m \cdot s^{-1}$. This velocity was chosen with sufficient distance to the choking velocity to ensure stable solids transport and to keep particle attrition low during the tests. The pressure drop in the bubbling fluidized bed was set by the amount of solids in the column to a value of either 15 or 20 mbar at the level of the column outlet without solids circulation to investigate the effect of the bed pressure drop on the operating behavior of the L-Valve and the gas leakage within the system. The L-Valve aeration was increased in several steps and the solids circulation rate was determined for each aeration by using the measurement cone described in the experimental setup section. The reported solids flux values refer to the cross section of the L-Valve and are averaged over three measurements. For the determination of the gas leakage, the propane concentration in the column was set to 1 percent, which is in adequate distance to the explosion limit of 1.7 percent. Thus, it was assured that no ignitable mixture can form in any section of the cold flow model. During operation of the cold flow model, the propane concentration was measured in the transporting section of the riser and the amount of leakage was calculated under the assumption that the complete L-Valve aeration adds to the riser aeration. The measured results were compared with equations from literature, as shown in the following section.

3. RESULTS AND DISCUSSION

Fig. 3 shows the solids circulation rate over the L-Valve aeration. Two different bed pressure drops were investigated and it is obvious, that the L-Valve operated at a higher bed pressure requires a lower aeration to achieve the same solids circulation rate. The reason for this behaviour is most likely the higher gas slip from the column through the moving bed in the standpipe, which supports the L-Valve aeration. For a bed pressure drop of 20 mbar, a maximum solids flux of 62 $kg \cdot m^{-2} \cdot s^{-1}$ was reached at an aeration rate of 1400 $l \cdot h^{-1}$. At higher aerations, a decrease of the solids circulation was observed. The differential pressure within the standpipe for both experiments is shown in Fig. 4, whereby positive values indicate higher absolute pressure at the top of the standpipe. With increasing solids circulation, an almost linear drop can be observed and a differential pressure of -11 mbar was reached for the 15 mbar bed pressure operation. It is commonly accepted, that if the pressure drop within the standpipe reaches that of a fluidized bed with the same height, the moving bed in the standpipe switches to a fluidized bed and the maximum solid circulation rate of the L-Valve is reached. However, if calculated for the used standpipe, this critical differential pressure is by a factor of four higher than what was reached in the experiments. This indicates, that the supply of solids from the fluidized bed via the inclined outlet was insufficient and higher solids circulation rates might be possible with a different outlet design. Similar limitations were observed by other researchers, although solids hoppers were used instead of a fluidized bed column (Geldart & Jones, 1991).

The backpressure of the L-Valve which is causing the standpipe pressure decrease in this model is mainly the sum of the pressure in the horizontal leg and the pressure in the transport section of the riser. The differential pressure in the horizontal leg is shown in Fig. 5. As can be expected, the pressure behaviour of this section is a function of the solids flux and not influenced by the pressure of the fluidized bed above. It can be seen, that after the required pressure threshold is reached to start the solids circulation, the additional backpressure of the horizontal section is rather low. Several equations exist for describing the pressure drop in the horizontal section of an L-Valve, and a comparison with the equation of Arena et.al. (Arena et al., 1998) showed excellent correlation. The pressure drop in the transporting section of the riser is shown in Fig. 6. For this chart, the pressure drop of the empty riser section was subtracted to determine the solids pressure drop. A linear function can be assumed for almost the complete region, which can be of use for a feedback control for the solids circulation rate in such systems.

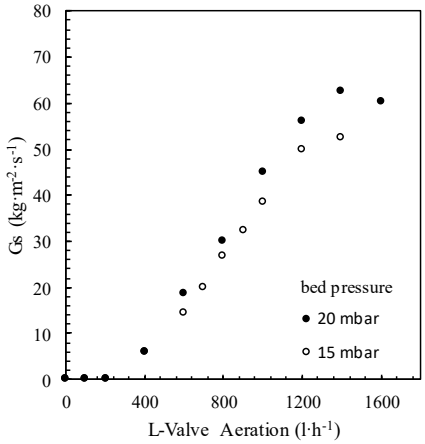

Fig. 3 L-Valve conveying behavior for different bed pressure drops

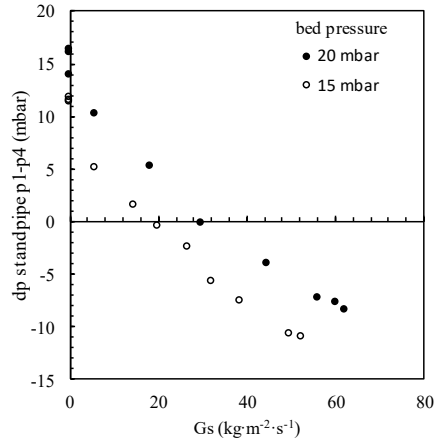

Fig. 4 Pressure drop in the standpipe

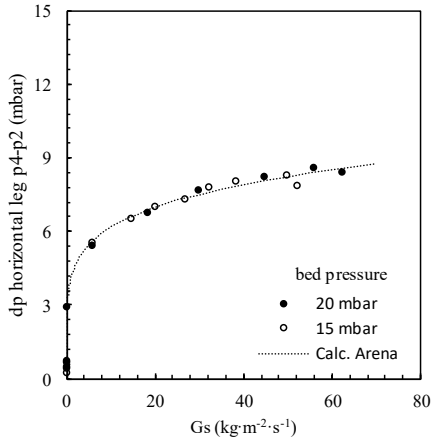

Fig. 5 Pressure drop in the horizontal leg of the L-Valve

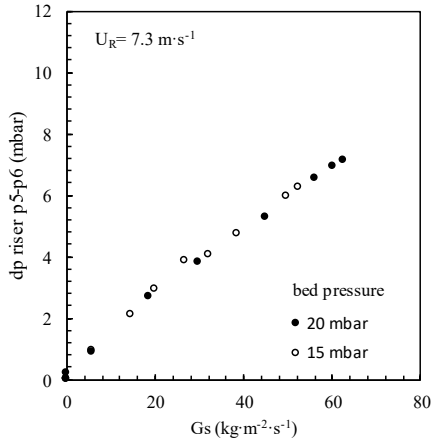

Fig. 6 Solids pressure drop in the transporting section of the riser

Fig. 7 and Fig. 8 show the gas leakage from the column into the riser system without solids circulation. As was shown in the previous tests, the pressure gradient between the outlet of the column and the riser is highest at this point due to the absence of solids in the transport section of the riser. Thus, the highest gas slip can be assumed for this operation condition, which was estimated by using the Ergun equation, Eq. (1). For the calculation, the pressure difference and the length between the exit of the column and the end of the horizontal section of the L-valve was used. Further, a constant porosity in these sections was assumed, namely the porosity at minimum fluidization conditions. The calculated values for the gas flow through the fixed bed are shown in Fig. 7 and Fig. 8 as theoretical leakage. This calculated leakage shows excellent correlation with the measured values, but can only be compared to the data point where no purge gas was used.

$$\frac{\Delta p}{L} = 150 \cdot \frac{(1-\varepsilon)^2}{\varepsilon^3} \cdot \frac{\mu \cdot U}{d_{sv}^2} + 1.75 \cdot \frac{1-\varepsilon}{\varepsilon^3} \cdot \frac{\rho_g \cdot U^2}{d_{sv}} \qquad (1)$$

By introducing purge gas in the top section of the standpipe, a linear decrease of the gas slip and the pressure drop between purge point and fluidized bed was observed. The leakage was reduced to values below the detection limit after the pressure drop in this section was passing zero, e.g. the pressure at the purge point was higher than the pressure at the column outlet. At all purge gas aerations, no solids circulation occurred.

As expected from the pressure profiles, the required amount of purge gas to seal the column is increasing with the pressure gradient between column and riser.

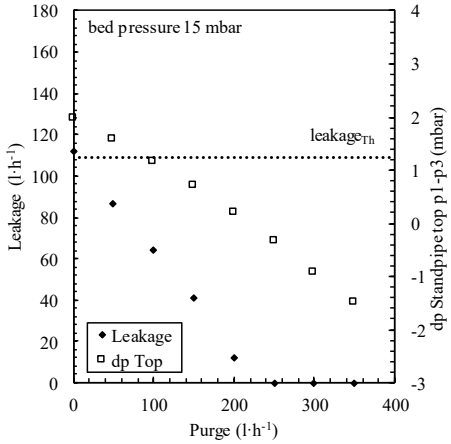

Fig. 7 Effect of purge gas without solids circulation at 15 mbar bed pressure

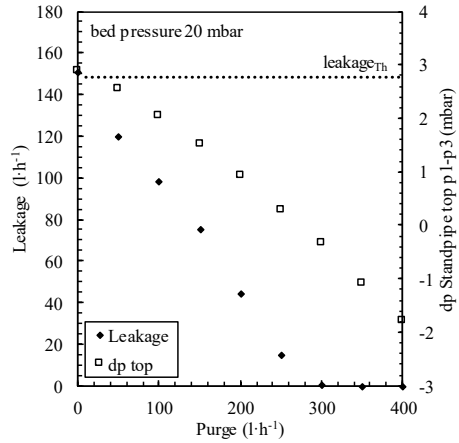

Fig. 8 Effect of purge gas without solids circulation at 20 mbar bed pressure

In a next step, the leakage behaviour of the system with solids circulation was investigated. Fig. 9 shows the gas leakage and standpipe pressure curve with solids circulation for a bed pressure of 15 mbar. As expected from the previous measurements, the gas leakage reached the highest values for operation without solids circulation and decreases significantly with rising L-Valve areation. As reported by Geldart (Geldart & Jones, 1991), the gas slip in the standpipe of the L-Valve is zero, if the velocity of the solids moving downwards and the gas velocity upwards through the moving bed are equal and opposite directed. The gas velocity trough the moving bed can again be calculated by the Ergun equation but has to take into account the bed porosity as shown by Geldart (Geldart & Jones, 1991). For the 15 mbar bed pressure, this point can be placed between the L-Valve aerations of 800 and 900 l·h^{-1} and is shown in the diagram as the dotted theoretical zero leakage line. Also the measured gas leakage was lowered below the detection limit between these operation points. For a L-Valve aeration of 600 l·h^{-1} it was shown, that a purge of 50 l·h^{-1} significantly reduces the gas leakage and 100 l·h^{-1} is sufficient to seal the L-Valve. The Effect of the purge gas on the solids transport rate was negligible.

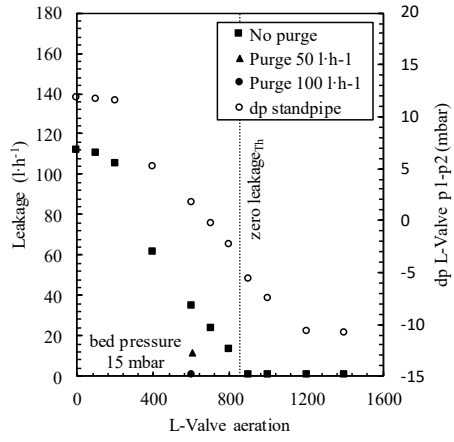

Fig. 9 Leakage behavior with solids circulation and 15 mbar bed pressure

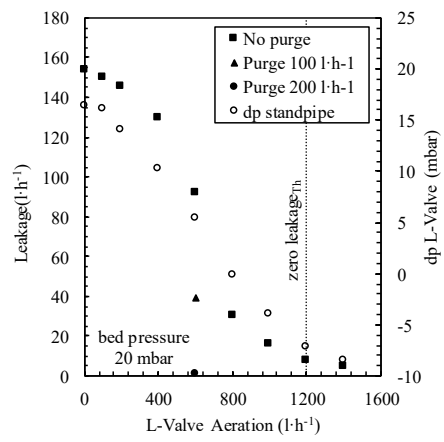

Fig. 10 Leakage behavior with solids circulation and 20 mbar bed pressure

Fig. 10 shows the gas slip in the system with a bed pressure drop of 20 mbar. Leakage values for this operating conditions are in general higher compared to the 15 mbar experiment. For the 600 $l \cdot h^{-1}$ L-Valve aeration point, 200 $l \cdot h^{-1}$ of purge gas were required to seal the system. The required sealing criteria was achieved at L-Valve aerations around 1200 $l \cdot h^{-1}$. However, the difference between calculated gas and solids velocities were small for the higher aeration rates and still a small gas leakage of around 5 $l \cdot h^{-1}$ was detected.

4. CONCLUSIONS

For CO_2 capture and storage, high demands on the CO_2 purity require a sufficient gas sealing at the outlet of the adsorber column. In this work, solids and gas flow characteristics of a L-Valve were investigated for different operating conditions. The L-vale was used to transport solids from a fluidized bed column to a riser and the resulting pressure conditions that determine the gas slip in the system were investigated. The gas leakage from the column trough the L-Vale into the riser was measured, whereby a flame ionisation detector proved to be a suitable measurement instrument for the detection of this gas slip. The following conclusions can be drawn:

- The gas leakage reaches the highest levels, if the solid circulation is stopped. This is mainly due to the absence of the solids pressure drop in the transport section of the riser. This leakage can be calculated with good agreement by using the Ergun equation. Purge gas can be used to eliminate this leakage, whereby the amount of purge gas required depends on the differential pressure between purge gas tap and the top of the standpipe.
- With rising solids circulation rate, the amount of leakage decreases and at certain operating conditions the L-vale aeration is stopping the gas leakage. This occurs, if the interstitial velocity of the gas moving up relative to the solids is equal or greater than the velocity of the solids moving downwards. However, if the solids pressure of the fluidized bed on the L-Valve standpipe is too high, this operating condition might not be reached.
- If the system is operated with lower solids circulation rate than required for the L-Valve aeration to eliminate gas slip, the gas purge can be used to stop the leakage. The required amount of purge gas is again connected to the differential pressure between purge gas introduction point and the top of the standpipe.

The differential pressure between the outlet of the column and the riser, which is the driving force for the gas leakage. This pressure can be altered by constructive measures like the height of the riser pot or operating measures, like the riser gas velocity. The results of this work showed, that by using a L-Valve in combination with a purge gas tap in the upper section of the standpipe, gas leakage can be avoided for a broad field of operating conditions.

ACKNOWLEDGEMENTS

This work was part of the Austrian Governments Climate and Energy Fund Project ViennaGreenCO2 No. 845022 coordinated by Technische Universität Wien. Financial support given by the Climate and Energy Fund is gratefully acknowledged.

Furthermore, the authors gratefully acknowledge funding and publication permission from Shell Global Solutions International BV, The Hague

NOTATION

d_{sv}	particle diameter (µm)
g	gravitational constant ($m \cdot s^{-2}$)
L	packed bed length (m)
Δp	differential pressure (mbar)
U	superficial gas velocity ($m \cdot s^{-1}$)
U_{mf}	minimal fluidization velocity ($m \cdot s^{-1}$)

Greek letters

ε_{mf}	bed voidage at minimum fluidization velocity (-)
ρ_g	gas density ($kg \cdot m^{-3}$)
ρ_p	particle density ($kg \cdot m^{-3}$)
ρ_b	bulk density ($kg \cdot m^{-3}$)
µ	gas viscosity ($kg \cdot m^{-1} \cdot s^{-1}$)

REFERENCES

Arena, U., Langeli, C. B., & Cammarota, A. (1998). L-valve behaviour with solids of different size and density. *Powder Technology*, *98*(3), 231–240. http://doi.org/10.1016/S0032-5910(98)00058-8

Chovichien, N., Pipatmanomai, S., & Chungpaibulpatana, S. (2013). Estimate of solids circulation rate through an L-valve in a CFB operating at elevated temperature. *Powder Technology*, *235*, 886–900. http://doi.org/10.1016/j.powtec.2012.11.016

Forbes, S. M., Verma, P., Curry, T. E., Friedmann, S. J., & Wade, S. M. (2008). *CCS Guidelines Guidelines for Carbon Dioxide Capture, Transport, and Storage*. *World Resources Institute*. http://doi.org/20113082154

Geldart, D. (1973). Types of gas fluidization. *Powder Technology*, *7*(5), 285–292. http://doi.org/10.1016/0032-5910(73)80037-3

Geldart, D., & Jones, P. (1991). The behaviour of L-valves with granular powders. *Powder Technology*, *67*(2), 163–174. http://doi.org/10.1016/0032-5910(91)80153-A

IPCC Special Report on Carbon Dioxide Capture and Storage. (2005). *Environmental Science and Technology* (Vol. 45). Cambridge University Press, Cambridge. http://doi.org/10.1021/es200619j

Knowlton, T. M., & Hirsan, I. (1978). L-Valves Characterized for Solids Flow. *Hydrocarbon Processing*, *57*(3), 149–156.

Krutka, H., Sjostrom, S., Starns, T., Dillon, M., & Silverman, R. (2013). Post-Combustion CO2 Capture Using Solid Sorbents: 1 MWe Pilot Evaluation. *Energy Procedia*, *37*, 73–88. http://doi.org/10.1016/j.egypro.2013.05.087

Nelson, T. O., Coleman, L. J. I., Kataria, A., Lail, M., Soukri, M., Quang, D. V., & Zahra, M. R. M. A. (2014). Advanced solid sorbent-based CO2 capture process. *Energy Procedia*, *63*, 2216–2229. http://doi.org/10.1016/j.egypro.2014.11.241

Pröll, T., Schöny, G., Sprachmann, G., & Hofbauer, H. (2016). Introduction and evaluation of a double loop staged fluidized bed system for post-combustion CO2 capture using solid sorbents in a continuous temperature swing adsorption process. *Chemical Engineering Science*, *141*, 166–174. http://doi.org/10.1016/j.ces.2015.11.005

Schöny, G., Dietrich, F., Fuchs, J., Pröll, T., & Hofbauer, H. (2016). A multi-stage fluidized bed system for continuous CO2 capture by means of temperature swing adsorption – first results from bench scale experiments.

Schöny, G., Zehetner, E., Fuchs, J., Pröll, T., Sprachmann, G., & Hofbauer, H. (2016). Design of a bench scale unit for continuous CO2 capture via temperature swing adsorption—Fluid-dynamic feasibility study. *Chemical Engineering Research and Design*, *106*, 155–167. http://doi.org/10.1016/j.cherd.2015.12.018

Sim, S., Cole, I. S., Choi, Y. S., & Birbilis, N. (2014). A review of the protection strategies against internal corrosion for the safe transport of supercritical CO2 via steel pipelines for CCS purposes. *International Journal of Greenhouse Gas Control*, *29*, 185–199. http://doi.org/10.1016/j.ijggc.2014.08.010

Yang, W. C., & Knowlton, T. M. (1993). L-valve equations. *Powder Technology*, *77*(1), 49–54. http://doi.org/10.1016/0032-5910(93)85006-U

Yazdanpanah, M. M., Forret, A., Gauthier, T., & Delebarre, A. (2012). An experimental investigation of L-valve operation in an interconnected circulating fluidized bed system. *Powder Technology*, *221*, 236–244. http://doi.org/10.1016/j.powtec.2012.01.007

Yazdanpanah IFP, M.-M., Ali Hoteit, F., Forret, A., Gauthier, T., Delebarre, A., Yazdanpanah, M.-M., & Hoteit, A. (2013). Gas Tracer Study in a Non Mechanical L-Valve, *7*. Retrieved from http://dc.engconfintl.org/cfb10